HEMATOLOGY, TRANSFUSION AND CELL THERAPY

www.htct.com.br

Original article

Exploring redox vulnerabilities in JAK2^{V617F}-positive cellular models

Keli Lima, *Lucia Rossetti Lopes*, *João Agostinho Machado-Neto* *

Biomedical Sciences Institute, Universidade de São Paulo, São Paulo, SP, Brazil

ARTICLE INFO

Article history:
Received 31 March 2020
Accepted 15 August 2020
Available online 13 September 2020

Keywords:
Myeloproliferative neoplasms
DUOXes
Redox signaling
NADPH oxidase
Ruxolitinib

ABSTRACT

Background: In Philadelphia chromosome-negative myeloproliferative neoplasm (MPN) models, reactive oxygen species (ROS) are elevated and have been implicated in genomic instability, JAK2/STAT signaling amplification, and disease progression. Although the potential effects of ROS on the MPN phenotype, the effects of ruxolitinib treatment on ROS regulation have been poorly explored. Herein, we have reported the impact of ruxolitinib on redox signaling transcriptional network, and the effects of diphenyleneiodonium (DPI), a pan NOX inhibitor, in JAK2^{V617F}-driven cellular models.

Method: Redox signaling-related genes were investigated in SET2 cells upon ruxolitinib treatment by RNA-seq (GEO accession GSE69827). SET2 and HEL cells, which represent JAK2^{V617F}-positive MPN cellular models with distinct sensitivity to apoptosis induced by ruxolitinib, were used. Cell viability was evaluated by MTT, apoptosis by annexin V/PI and flow cytometry, and cell signaling by quantitative PCR and Western blot.

Main results: Ruxolitinib impacted on a network composed of redox signaling-related genes, and *DUOX1* and *DUOX2* were identified as potential modulators of ruxolitinib response. In SET2 and HEL cells, DPI reduced cell viability and, at low doses, it significantly potentiated ruxolitinib-induced apoptosis. In the molecular scenario, DPI inhibited STAT3, STAT5 and S6 ribosomal protein phosphorylation and induced PARP1 cleavage in JAK2^{V617F}-positive cells. DPI combined with ruxolitinib increased PARP1 cleavage in SET2 cells and potentiated ruxolitinib-reduced STAT3, STAT5 and S6 ribosomal protein in HEL cells.

Conclusion: Our study reveals a potential adaptation mechanism for resistance against ruxolitinib by transcriptionally reprogramming redox signaling in JAK2^{V617F} cells and exposes redox vulnerabilities with therapeutic value in MPN cellular models.

* *Corresponding author at*: Department of Pharmacology, Institute of Biomedical Sciences of University of São Paulo, Av. Prof. Lineu Prestes, 1524, CEP 05508-900, São Paulo, SP, Brazil.
E-mail address: jamachadoneto@usp.br (J.A. Machado-Neto).

https://doi.org/10.1016/j.htct.2020.08.006

Introduction

Philadelphia chromosome-negative myeloproliferative neoplasms (MPN) display aberrant proliferation of myeloid progenitors that retain differentiation capacity and have heightened risk of bone marrow failure or acute myeloid leukemia transformation.[1,2] JAK2 activating mutations (*i.e.* JAK2^{V617F}, *indel* CALR, and MPL mutations) are highly present in the most frequent MPN, including essential thrombocythemia, polycythemia vera (PV), and primary myelofibrosis (PMF), which has been targeted by ruxolitinib, a selective JAK1/2 inhibitor.[3] Despite some clinical benefits of ruxolitinib treatment in intermediate and high-risk PMF and PV patients, the drug does not lead to complete remission and elimination of the mutated clone.[4,5] Altogether, a better understanding of the adaptive processes of the neoplastic clone in the face of inhibition of JAK2, the central signaling pathway involved in the malignant characteristics of MPN is necessary.

The role of regulation of reactive oxygen species (ROS) in MPN models has been the subject of debate.[6] In the murine model, the JAK2^{V617F} mutation is able to induce ROS production, which leads to genomic instability and disease progression.[7] In humans, baseline levels of ROS are increased in hematopoietic cells from MPN patients when compared to healthy individuals.[8,9] From a molecular point of view, increased levels of ROS may inhibit protein phosphatases and participate in the amplification of the JAK2-mediated signaling pathway.[7]

In the present study, we investigated the impact of the ruxolitinib treatment on a network composed of redox signaling-related genes in a JAK2^{V617F} cell model, and *DUOX1* and *DUOX2* were identified as potential modulators of ruxolitinib response. DUOXes are isoenzymes that belong to the NADPH oxidase family (NOX1-5 and DUOX1-2) and are dedicated ROS generating enzymes.[10,11] Since there are no selective inhibitors for DUOXes,[12] diphenyleneiodonium (DPI), a pan NOX/DUOX inhibitor,[13] was used for pharmacological intervention. Herein, we also described the molecular and cellular effects of the treatment with DPI on cell survival and response to ruxolitinib in JAK2^{V617F}-positive cellular models.

Material and methods

RNA-seq data analysis

RNA-seq data were obtained from Meyer et al.[14] (https://www.ncbi.nlm.nih.gov/geo; GEO accession GSE69827). The expression of 81 redox signaling-related genes in samples from naïve SET2 cells (GSM1817344, GSM1817345, and GSM1817346) and ruxolitinib-treated SET2 cells (GSM1817332, GSM1817333, and GSM1817334) was investigated. Gene expression was expressed as a fold change of the mean of normalized counts of naïve SET2 cells, which was set as 1. Genes that presented mean ≥2-fold either direction were included in the heatmap using multiple experiment viewer (MeV) 4.9.0 software (http://mev.tm4.org). Genes with counts = 0 in any condition were excluded from the heatmap. Network construction was performed using modulated genes and the GeneMANIA database (https://genemania.org/). The full list of genes included, normalized counts, and relative expression values are described in Supplementary Table 1.

Cell culture and inhibitors

SET2 cells were kindly provided by Prof. Fabíola Attié de Castro (School of Pharmaceutical Sciences of Ribeirão Preto, University of São Paulo, Ribeirão Preto, Brazil). HEL was obtained from ATCC (Philadelphia, PA, USA). SET2 and HEL cells harboring JAK2^{V617F} mutation were tested and authenticated by Short Tandem Repeat (STR) matching analysis using the PowerPlex® 16 HS system (Promega, Madison, WI, USA) and the ABI 3500 Sequence Detector System (Life Technologies, Foster City, CA, USA). Cell culture conditions were performed following the recommendations of ATCC and DSMZ. All cell lines were mycoplasma free. Ruxolitinib was obtained from InvivoGen (San Diego, CA, USA). Diphenyleneiodonium chloride (DPI) was obtained from Sigma-Aldrich (St. Louis, MO, USA). Ruxolitinib and DPI doses used in functional assays were selected based on previous studies.[15–17]

Quantitative PCR (qPCR)

Total RNA from SET2 cells treated with vehicle or ruxolitinib (100, 300, and 1000 nM) was obtained using TRIzol reagent (Thermo Fisher Scientific). cDNA was synthesized from 1 μg of RNA using High-Capacity cDNA Reverse Transcription Kit (Thermo Fisher Scientific). Quantitative PCR (qPCR) was performed with an ABI 7500 Sequence Detector System using SyberGreen System for *DUOX1* (FW: TTCACGCAGCTCTGTGTCAA; RV: AGGGACAGATCATATCCTGGCT) or *DUOX2* (FW: ACGCAGCTCTGTGTCAAAGGT; RV: TGATGAACGAGACTCGACAGC). *ATCB* (FW: AGGCCAACCGCGAGAAG; RV: ACAGCCTGGATAGCAACGTACA) and *HPRT1* (FW: GAACGTCTTGCTCGAGATGTGA; RV: TCCAGCAGGTCAGCAAAGAAT) were the reference genes. The relative quantification value was calculated using the equation $2^{-\Delta\Delta CT}$.[18] A negative 'No Template Control' was included for each primer pair.

Cell viability assay

Cell viability was measured through methylthiazoletetrazolium (MTT) assay. SET2 (4×10^4 cells/well) and HEL cells (2×10^4 cells/well) were cultured in a 96-well plate in RPMI medium containing 10% or 20% FBS, respectively, in the presence of vehicle or increasing concentrations of DPI (0.1, 0.25, 0.5, 1, 2.5, 5 and 10 μM) for 48 h. DMSO (Ø) was used as a negative control. IC_{50} values were calculated using nonlinear regression analysis on GraphPad Prism 5 (GraphPad Software, Inc., San Diego, CA, USA).

Apoptosis assay

SET2 and HEL were seeded in 24-well plates and treated with vehicle, DPI (5 or 10 μM), ruxolitinib (300 nM) or DPI (5 or 10 μM) plus ruxolitinib (300 nM) for 48 h. Cells were then washed twice with ice-cold PBS and resuspended in binding buffer containing 1 μg/mL propidium iodide and 1 μg/mL APC-labeled annexin V. All specimens were acquired by flow cytometry

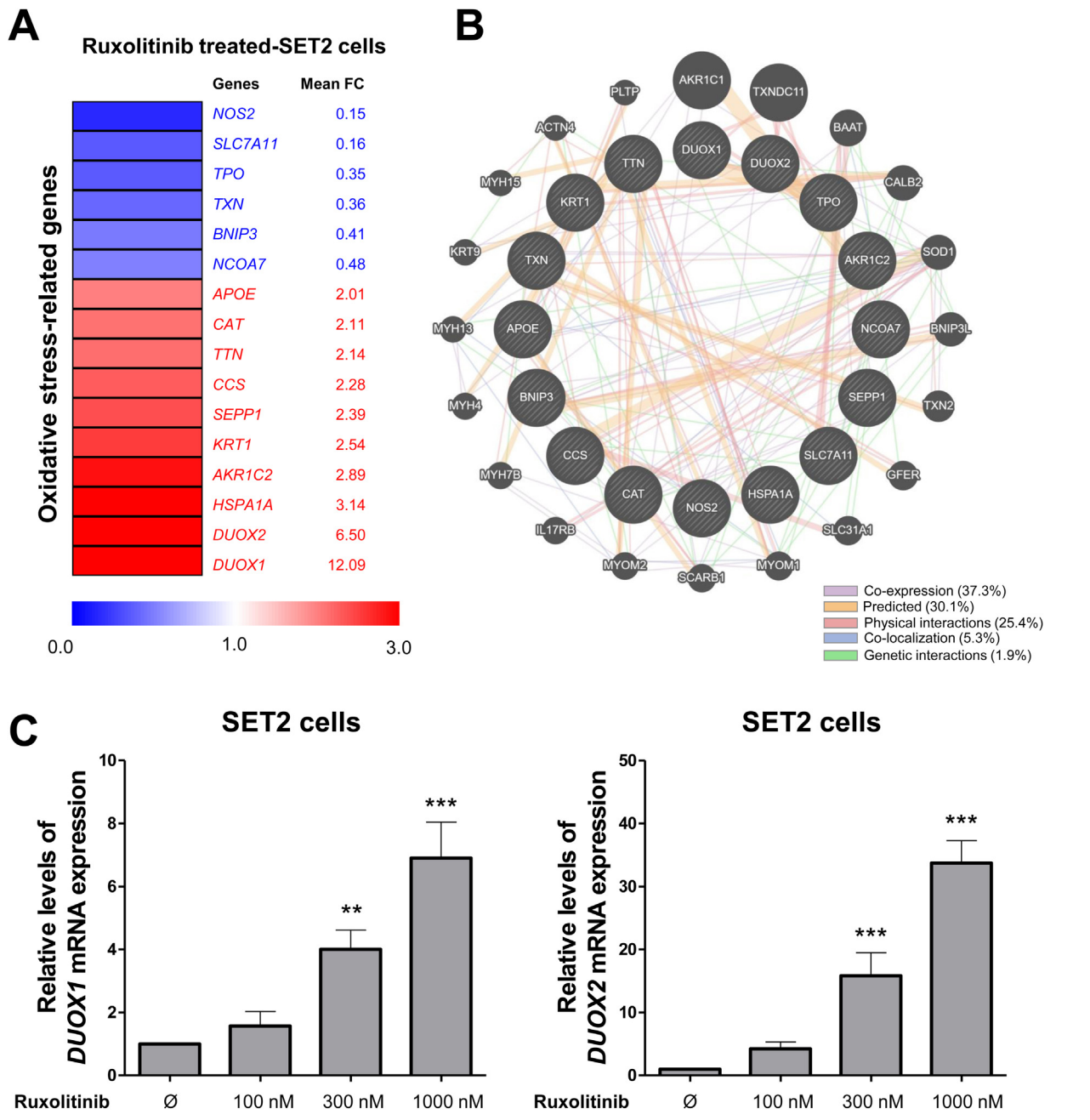

Figure 1 – Ruxolitinib increases DUOX signaling in SET2 cells. (A) Gene expression heatmap from RNA-seq analysis of SET2 cells upon the treatment with ruxolitinib. Data was obtained from Meyer et al.[14] (GEO accession GSE69827). Gene expression was expressed as fold change of the mean of normalized counts of naïve SET2 cells, which was set as 1; genes demonstrating ≥2-fold in either direction are included in the heatmap. The mean of fold change obtained from three experimental replicates is indicated. (B) Network for redox signaling-related genes constructed using the GeneMANIA database. The up- and down-regulated genes in RNAseq analysis are illustrated as crosshatched circles and the interacting genes included by modeling the software are indicated by circles without crosshatched. The main biological interactions between genes are indicated by colored lines and are described in the Figure. (C) qPCR analysis of *DUOX1* and *DUOX2* mRNA expression in SET2 cells treated with increasing concentrations of ruxolitinib (vehicle, 100, 300, or 1000 nM) for 48 h. Bar graphs represent the mean ± SD of three independent experiments. The *p* values are indicated in the graphs; $^{**}p < 0.01$, $^{***}p < 0.0001$; ANOVA test and Bonferroni post-test.

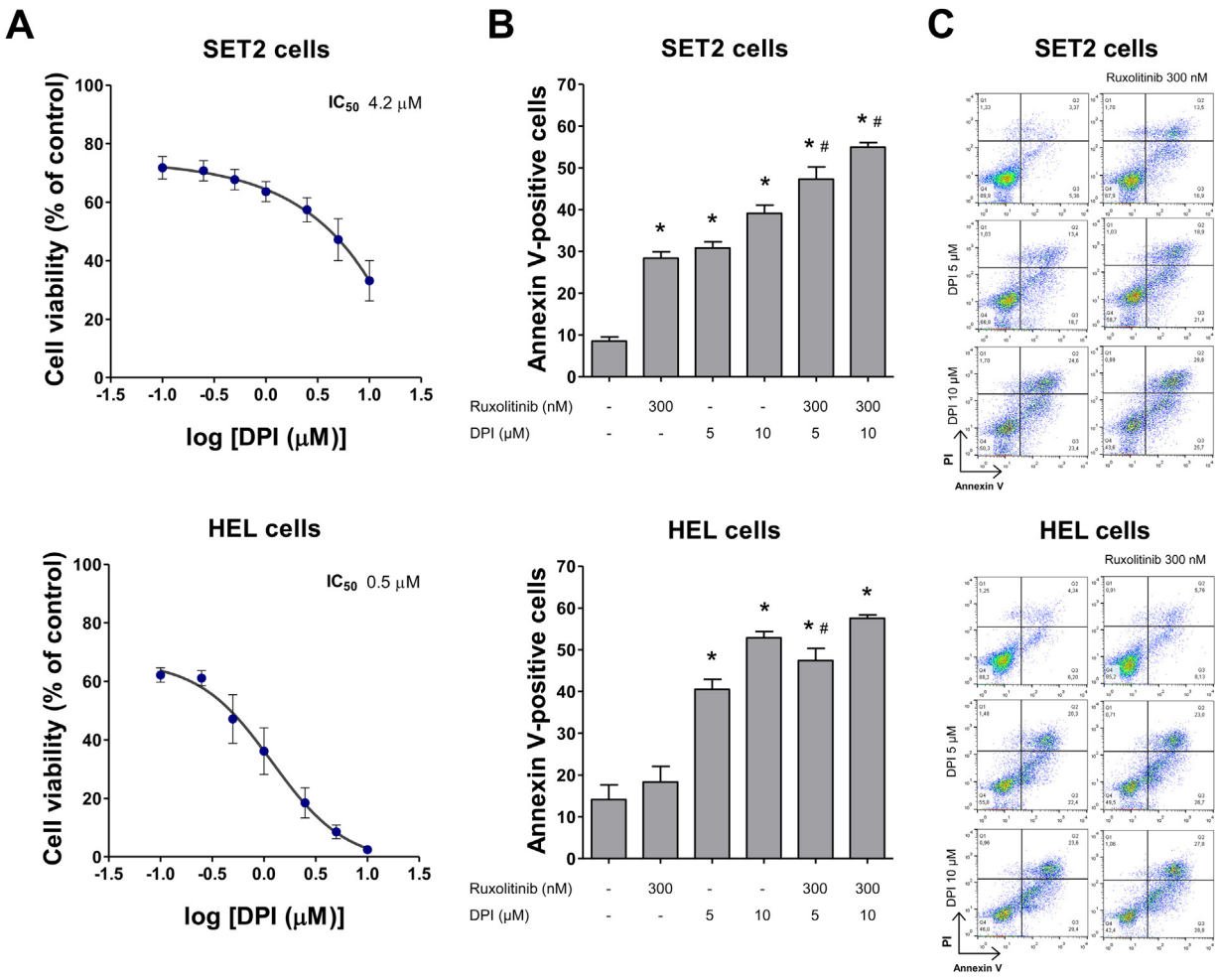

Figure 2 – NADPH oxidase inhibition by DPI potentiates ruxolitinib-induced apoptosis in SET2 and HEL cells. (A) Dose-response cytotoxicity was analyzed by methylthiazoletetrazolium (MTT) assay for SET2 and HEL cells treated with vehicle or increasing concentrations of diphenyleneiodonium (DPI; 0.1, 0.25, 0.5, 1, 2.5, 5, and 10 μM) for 48 h. Values are expressed as the percentage of viable cells relative to vehicle-treated controls. Results are shown as the mean ± SD of at least three independent experiments. (B) Apoptosis was detected by flow cytometry in HEL or SET2 cells treated with vehicle or DPI (5 or 10 μM) and/or ruxolitinib (300 nM) for 48 h using an annexin V/PI staining method. Representative dot plots are shown for each condition; the upper and lower right quadrants (Q2 plus Q3) cumulatively contain the apoptotic population (annexin V + cells). (C) Bar graphs represent the mean ± SD of at least three independent experiments quantifying apoptotic cell death. The *p* values and cell lines are indicated in the graphs. **p* < 0.05 for DPI- and/or ruxolitinib-treated cells *vs.* untreated cells, #*p* < 0.05 for DPI- or ruxolitinib-treated cells *vs.* combination treatment at the corresponding doses; ANOVA test and Bonferroni post-test, all pairs were analyzed and statistically significant differences are indicated.

(FACSCalibur; Becton Dickinson) after incubation for 15 min at room temperature in a light-protected area and analyzed using FlowJo software (Treestar, Inc., San Carlos, CA, USA).

Western blot analysis

SET2 and HEL were treated with vehicle, DPI (5 μM) and/or ruxolitinib (300 nM) for 24 h. Equal amounts of protein were used as total extracts, followed by SDS-PAGE, Western blot analysis with the indicated antibodies and imaging using the SuperSignal™ West Dura Extended Duration Substrate System (Thermo Fisher Scientific, San Jose, CA, USA) and G:BOX Chemi XX6 gel doc systems (Syngene, Cambridge, UK). Antibodies against p-STAT3^{Y705} (#9131S), STAT3 (#4904), p-STAT5^{Y694} (#9359S), STAT5 (#25656), p-ERK1/2$^{T202/Y204}$ (#9101), ERK1/2 (#9102), p-S6 ribosomal protein$^{S235/S26}$ (#4858), S6 ribosomal protein (#2217), PARP1 (#9542), and α-tubulin (#2144) were obtained from Cell Signaling Technology (Danvers, MA, USA).

Statistical analysis

Statistical analyses were performed using GraphPad Prism 5 (GraphPad Software, Inc.). For comparisons, ANOVA test and Bonferroni post-test or Student *t*-test were used. A *p*-value <0.05 was considered as statistically significant. All pairs were analyzed and statistically significant differences are indicated.

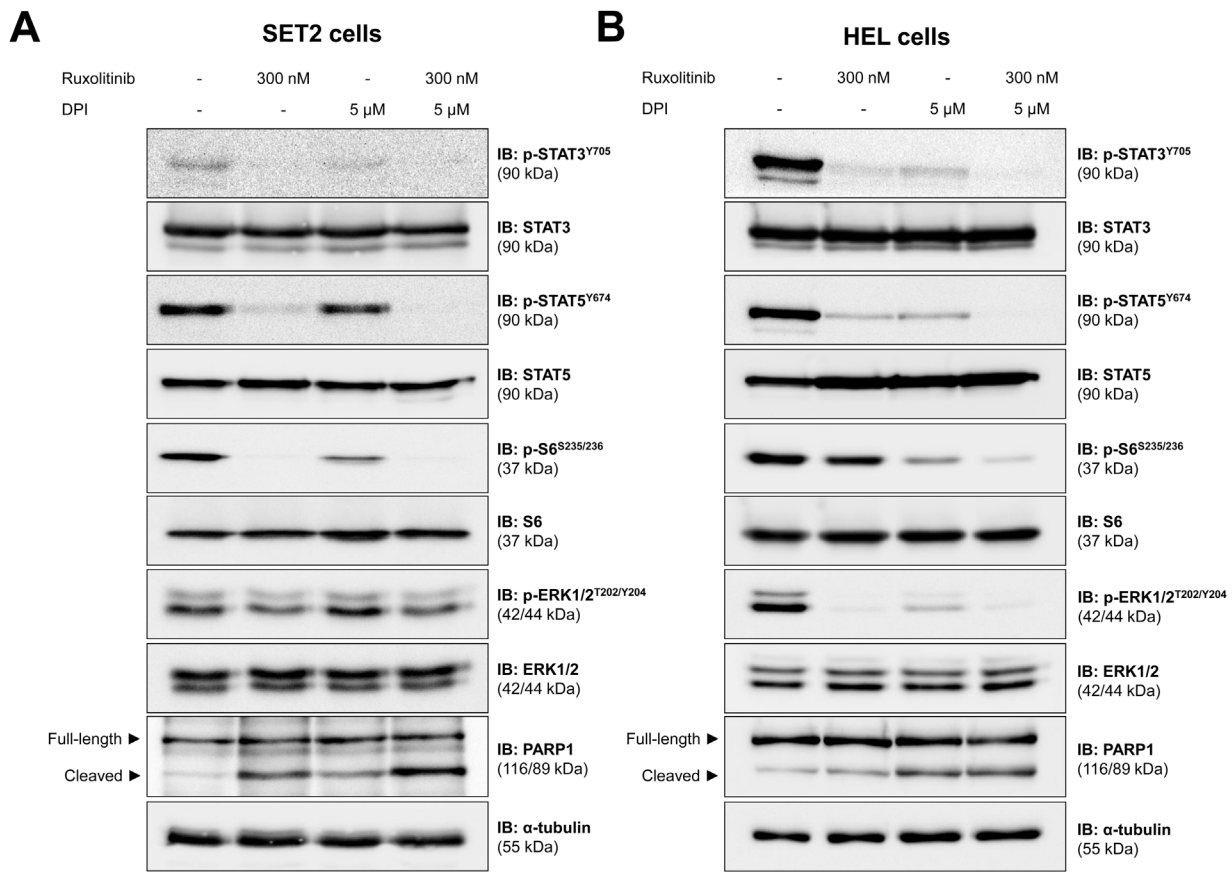

Figure 3 – NADPH oxidase regulates JAK2/STAT redox signaling pathways in JAK2^{V617F}-positive cell lines. Western blot analysis for p-STAT3^{Y705}, p-STAT5^{Y694}, p-ERK1/2$^{T202/Y204}$, p-S6 ribosomal protein$^{S235/S26}$, and PARP1 (total and cleaved) in total cell extracts from SET2 (A) and HEL (B) cells treated with vehicle or diphenyleneiodonium (DPI. 5 μM) and/or ruxolitinib (300 nM); membranes were reprobed with the antibody for the detection of the respective total protein or α-tubulin, and revealed with the SuperSignal™ West Dura Extended Duration Substrate system using a G:BOX Chemi XX6 gel doc systems.

Results

Ruxolitinib modifies genes involved in redox signaling network in SET2 cells

In order to identify redox vulnerabilities in MPN cells, we investigated the impact of ruxolitinib on the expression of redox signaling-related genes. Using the cutoff of 2-fold for either direction, 16 genes were found to be differentially expressed (6 downregulated and 10 upregulated) in SET2 upon ruxolitinib treatment for 48 h (Figure 1A). Network analysis indicated an intense biological association between modulated genes, including co-expression, predictive correlations, physical interactions, co-localization, and genetic interactions (Figure 1B). Since ROS production has been associated with malignant phenotype of MPN cells, the upregulation of *DUOX1* and *DUOX2* caught our attention and these genes were selected for validation using quantitative PCR. In SET2 cells, ruxolitinib increased in a dose-dependent manner *DUOX1* and *DUOX2* mRNA levels (Figure 1B,C).

NADPH oxidase inhibition by DPI reduces cell viability and potentiates ruxolitinib-induced apoptosis JAK2^{V617F} cells

Next, the cellular and molecular effects of DPI, a pan NOX/DUOX inhibitor, were investigated in MPN cellular models with distinct sensitivity to apoptosis induced by ruxolitinib, being SET2 cells more sensitive than HEL cells.[19,20] In both JAK2^{V617F} cell lines, DPI reduced cell viability, being more potent in HEL cells (Figure 2A). Using nonlinear regression analysis, the IC_{50} values for DPI at 48 h was 4.2 and 0.5 μM, in SET2 and HEL cells, respectively. Of note, low doses of DPI (5 μM) reduced cell survival and potentiated ruxolitinib-induced apoptosis in both cell lines, especially in SET2 cells (all $p < 0.05$) (Figure 2B,C).

DPI inhibits JAK2 downstream signaling pathway in SET2 and HEL cells

The effects of DPI alone and in combination with ruxolitinib in each cell line are corroborated in the molecular scenario. In SET2 cells, DPI weakly inhibited phosphoryla-

tion of STAT3, STAT5, and S6 ribosomal protein (an effector of the PI3K/AKT/mTOR pathway) and induces cleavage of PARP1, but did not modulate the activation of ERK1/2 (an effector of the MAPK pathway). The combination of DPI and ruxolitinib showed a higher PARP1 cleavage, as compared to monotherapy in SET2 cells (Figure 3A). On the other hand, the phosphorylation of STAT3, STAT5, S6 ribosomal protein, and ERK1/2 and the cleavage of PARP1 were strongly induced by DPI in HEL cells. In addition, the combination of DPI with ruxolitinib potentiated the inhibition of STAT3, STAT5, and S6 ribosomal protein in HEL cells (Figure 3B). Ruxolitinib treatment in monotherapy inhibited the JAK2/STAT and MAPK pathway in both cell lines, but only triggered PARP1 cleavage and strongly reduced S6 ribosomal protein phosphorylation in SET2 cells (Figure 3).

Discussion

Herein, we have reported the effects of ruxolitinib on the redox signaling network and the effects of DPI in JAK2^{V617F}-driven cellular models. There is evidence that excessive ROS production is involved in the proliferative advantage of MPN clones, and the decrease in ROS generation may prevent genomic instability and ultimately myelofibrotic and leukemia transformation.[7,21–23] Although the potential effects of ROS on the myeloproliferative phenotype, the effects of treatment with ruxolitinib on ROS regulation in MPN have been poorly explored.[24]

In the present study, ruxolitinib treatment impacted on transcriptional modulation of redox signaling-related genes in a JAK2^{V617F}-positive cell line, including a marked upregulation of *DUOX1* and *DUOX2*. DUOXes are the least characterized members of the family of NADPH oxidases, which are enzymes dedicated to the generation ROS that trigger multiple signaling pathways. Furthermore, DUOXes do not have selective inhibitors.[12] In solid tumors, DUOX1 and DOUX2 expression are frequently deregulated and their clinical significance seems to be tissue-specific.[25]

DPI, diphenyleneiodonium, is widely used as an inhibitor of flavoenzymes, such as NOXes and DUOXes.[10] In chronic myeloid leukemia, DPI reduces cell proliferation and clonogenicity *in vitro*, tumorigenesis *in vivo*, and synergizes with imatinib.[17] In BCR-ABL1-positive cells, DPI reduces the activation of PI3K/AKT/mTOR and MAPK pathway,[17,26] which corroborates our findings in JAK2^{V617F}-positive models. In primary MPN cells and SET2 cell line, vorinostat, an HDAC inhibitor, induces apoptosis in a mechanism dependent on reduction in intracellular levels of ROS, and also synergizes with agents that decrease ROS generation, including DPI.[27]

Although DUOXes were the modified enzymes in our initial analysis, the potential effect of DPI on other members of the NADPH oxidase family cannot be overlooked. In SET2 cells, *DUOX2* and *CYBB* (NOX2) are the predominant transcripts, followed by a low expression of *NOX5* and *DUOX1*. *NOX4* levels were not detected and there was no expression of *NOX1* and *NOX3* in the analysis using RNAseq (Supplementary Figure 1). The role of NOX2 has been widely explored in murine BCR-ABL1-positive leukemia and KRAS-driven MPN model: NOX2 deficiency reduces ROS levels, the proliferation of myeloid progenitors, and self-renewal programs.[28,29] Thus, the effects of DPI as a non-selective inhibitor for DUOXes and NOXes may be desired in this context. Together, these pieces of evidence suggest that MPN cells display "ROS addiction", as observed in other ROS-generating cancers,[30] which will contribute to the identification of new therapeutic targets and certainly improve the response to current therapies.

Conclusion

Our study reveals a potential adaptive mechanism in the resistance against ruxolitinib by transcriptionally reprogramming redox signaling in JAK2^{V617F} cells and exposes redox vulnerabilities with therapeutic value in MPN cellular models.

Authorship

K.L. participated in the acquisition, analysis of data, and draft of the article. L.R.L. participated in the conception of the study, interpretation of data, and revision of the article critically for important intellectual content. J.A.M.-N. participated in the conception and design of the study, acquisition, analysis, and interpretation of data, and draft the article. All authors approved the final version of the manuscript.

Conflict of interest disclosure

The authors declare no competing financial interests.

Acknowledgments

This study was supported by the São Paulo Research Foundation (FAPESP) [#2019/23864-7, #2013/07937-8] and Conselho Nacional de Desenvolvimento Científico e Tecnológico (CNPq) [#402587/2016-2]. LRL is a member of CEPID Redoxoma FAPESP.

Appendix A. Supplementary data

Supplementary material related to this article can be found, in the online version, at doi:https://doi.org/10.1016/j.htct.2020.08.006.

REFERENCES

1. Spivak JL. Myeloproliferative neoplasms. N Engl J Med. 2017;376:2168–81.
2. Thoennissen NH, Krug UO, Lee DH, Kawamata N, Iwanski GB, Lasho T, et al. Prevalence and prognostic impact of allelic imbalances associated with leukemic transformation of Philadelphia chromosome-negative myeloproliferative neoplasms. Blood. 2010;115:2882–90.
3. Grinfeld J, Nangalia J, Baxter EJ, Wedge DC, Angelopoulos N, Cantrill R, et al. Classification and personalized prognosis in myeloproliferative neoplasms. N Engl J Med. 2018;379:1416–30.
4. Harrison C, Kiladjian JJ, Al-Ali HK, Gisslinger H, Waltzman R, Stalbovskaya V, et al. JAK inhibition with ruxolitinib versus best available therapy for myelofibrosis. N Engl J Med. 2012;366:787–98.

5. Vannucchi AM, Kiladjian JJ, Griesshammer M, Masszi T, Durrant S, Passamonti F, et al. Ruxolitinib versus standard therapy for the treatment of polycythemia vera. N Engl J Med. 2015;372:426–35.
6. Machado-Neto JA, Traina F. Reactive oxygen species overload promotes apoptosis in JAK2V617F-positive cell lines. Rev Bras Hematol Hemoter. 2016;38:179–81.
7. Marty C, Lacout C, Droin N, Le Couedic JP, Ribrag V, Solary E, et al. A role for reactive oxygen species in JAK2 V617F myeloproliferative neoplasm progression. Leukemia. 2013;27:2187–95.
8. Vener C, Novembrino C, Catena FB, Fracchiolla NS, Gianelli U, Savi F, et al. Oxidative stress is increased in primary and post-polycythemia vera myelofibrosis. Exp Hematol. 2010;38:1058–65.
9. Hurtado-Nedelec M, Csillag-Grange MJ, Boussetta T, Belambri SA, Fay M, Cassinat B, et al. Increased reactive oxygen species production and p47phox phosphorylation in neutrophils from myeloproliferative disorders patients with JAK2 (V617F) mutation. Haematologica. 2013;98:1517–24.
10. Roy K, Wu Y, Meitzler JL, Juhasz A, Liu H, Jiang G, et al. NADPH oxidases and cancer. Clin Sci (Lond). 2015;128:863–75.
11. Weyemi U, Redon CE, Parekh PR, Dupuy C, Bonner WM. NADPH Oxidases NOXs and DUOXs as putative targets for cancer therapy. Anticancer Agents Med Chem. 2013;13:502–14.
12. Altenhofer S, Radermacher KA, Kleikers PW, Wingler K, Schmidt HH. Evolution of NADPH oxidase inhibitors: selectivity and mechanisms for target engagement. Antioxid Redox Signal. 2015;23:406–27.
13. Massart C, Giusti N, Beauwens R, Dumont JE, Miot F, Sande JV. Diphenyleneiodonium, an inhibitor of NOXes and DUOXes, is also an iodide-specific transporter. FEBS Open Bio. 2013;4:55–9.
14. Meyer SC, Keller MD, Chiu S, Koppikar P, Guryanova OA, Rapaport F, et al. CHZ868, a type II JAK2 inhibitor, reverses type I JAK inhibitor persistence and demonstrates efficacy in myeloproliferative neoplasms. Cancer Cell. 2015;28:15–28.
15. Fenerich BA, Fernandes JC, Rodrigues Alves AP, Coelho-Silva JL, Scopim-Ribeiro R, Scheucher PS, et al. NT157 has antineoplastic effects and inhibits IRS1/2 and STAT3/5 in JAK2(V617F)-positive myeloproliferative neoplasm cells. Signal Transduct Target Ther. 2020;5:5.
16. Machado-Neto JA, de Melo Campos P, Favaro P, Lazarini M, da Silva Santos Duarte A, Lorand-Metze I, et al. Stathmin 1 inhibition amplifies ruxolitinib-induced apoptosis in JAK2V617F cells. Oncotarget. 2015;6:29573–84.
17. Sanchez-Sanchez B, Gutierrez-Herrero S, Lopez-Ruano G, Prieto-Bermejo R, Romo-Gonzalez M, Llanillo M, et al. NADPH oxidases as therapeutic targets in chronic myelogenous leukemia. Clin Cancer Res. 2014;20:4014–25.
18. Livak KJ, Schmittgen TD. Analysis of relative gene expression data using real-time quantitative PCR and the 2(-Delta Delta C(T)) method. Methods. 2001;25:402–8.
19. Lima K, Carlos J, Alves-Paiva RM, Vicari HP, Souza Santos FP, Hamerschlak N, et al. Reversine exhibits antineoplastic activity in JAK2(V617F)-positive myeloproliferative neoplasms. Sci Rep. 2019;9:9895.
20. Machado-Neto JA, Fenerich BA, Scopim-Ribeiro R, Eide CA, Coelho-Silva JL, Dechandt CRP, et al. Metformin exerts multitarget antileukemia activity in JAK2(V617F)-positive myeloproliferative neoplasms. Cell Death Dis. 2018;9:311.
21. Yalcin S, Marinkovic D, Mungamuri SK, Zhang X, Tong W, Sellers R, et al. ROS-mediated amplification of AKT/mTOR signalling pathway leads to myeloproliferative syndrome in Foxo3(-/-) mice. EMBO J. 2010;29:4118–31.
22. Xu D, Zheng H, Yu WM, Qu CK. Activating mutations in protein tyrosine phosphatase Ptpn11 (Shp2) enhance reactive oxygen species production that contributes to myeloproliferative disorder. PLoS One. 2013;8:e63152.
23. Bjorn ME, Hasselbalch HC. The role of reactive oxygen species in myelofibrosis and related neoplasms. Mediators Inflamm. 2015;2015:648090.
24. Bjorn ME, Brimnes MK, Gudbrandsdottir S, Andersen CL, Poulsen HE, Henriksen T, et al. Ruxolitinib treatment reduces monocytic superoxide radical formation without affecting hydrogen peroxide formation or systemic oxidative nucleoside damage in myelofibrosis. Leuk Lymphoma. 2019;60:2549–57.
25. Little AC, Sulovari A, Danyal K, Heppner DE, Seward DJ, van der Vliet A. Paradoxical roles of dual oxidases in cancer biology. Free Radic Biol Med. 2017;110:117–32.
26. Naughton R, Quiney C, Turner SD, Cotter TG. Bcr-Abl-mediated redox regulation of the PI3K/AKT pathway. Leukemia. 2009;23:1432–40.
27. Cardoso BA, Ramos TL, Belo H, Vilas-Boas F, Real C, Almeida AM. Vorinostat synergizes with antioxidant therapy to target myeloproliferative neoplasms. Exp Hematol. 2019;72, 60-71 e11.
28. Adane B, Ye H, Khan N, Pei S, Minhajuddin M, Stevens BM, et al. The hematopoietic oxidase NOX2 regulates self-renewal of leukemic stem cells. Cell Rep. 2019;27, 238-254 e236.
29. Aydin E, Hallner A, Grauers Wiktorin H, Staffas A, Hellstrand K, Martner A. NOX2 inhibition reduces oxidative stress and prolongs survival in murine KRAS-induced myeloproliferative disease. Oncogene. 2019;38:1534–43.
30. Hole PS, Darley RL, Tonks A. Do reactive oxygen species play a role in myeloid leukemias? Blood. 2011;117:5816–26.